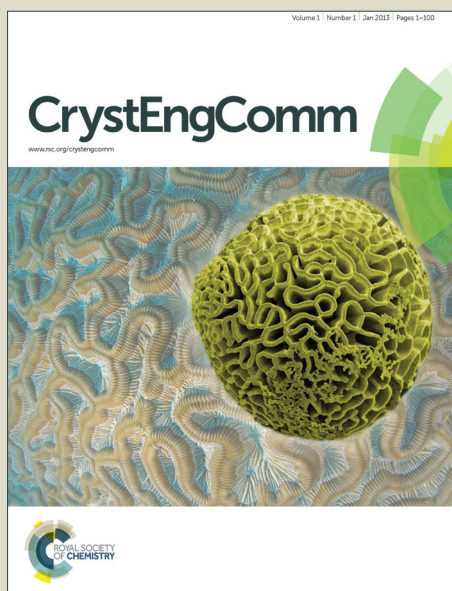


CrystEngComm

Accepted Manuscript



This is an *Accepted Manuscript*, which has been through the Royal Society of Chemistry peer review process and has been accepted for publication.

Accepted Manuscripts are published online shortly after acceptance, before technical editing, formatting and proof reading. Using this free service, authors can make their results available to the community, in citable form, before we publish the edited article. We will replace this *Accepted Manuscript* with the edited and formatted *Advance Article* as soon as it is available.

You can find more information about *Accepted Manuscripts* in the [Information for Authors](#).

Please note that technical editing may introduce minor changes to the text and/or graphics, which may alter content. The journal's standard [Terms & Conditions](#) and the [Ethical guidelines](#) still apply. In no event shall the Royal Society of Chemistry be held responsible for any errors or omissions in this *Accepted Manuscript* or any consequences arising from the use of any information it contains.

Cite this: DOI: 10.1039/c0xx00000x

www.rsc.org/xxxxxx

HIGHLIGHT**Soft-oxometalates beyond crystalline polyoxometalates: formation, structure and properties****Soumyajit Roy***Received (in XXX, XXX) Xth XXXXXXXXX 20XX, Accepted Xth XXXXXXXXX 20XX*

DOI: 10.1039/b000000x

Polyoxometalates (POMs) as the name suggests are single molecular charged or uncharged clusters comprising of many metal centres and oxygen atoms. They are crystalline. On the other hand, recently, a class of macroionic, superstructured assembly of POMs has been found which is reminiscent of soft matter and has been proposed to be called Softoxometalates (SOMs). This highlight gives a personal account of our work with SOMs. Starting with a brief background and history of SOMs we explore the reasons of their formation. Thereafter we discuss the charge regulation mechanism for the stabilization of SOMs. Few case studies for the directed formation of large surface area, mesoscopic SOMs are also discussed. Thereafter, we discuss the effects of sound and light on SOMs. This highlight finally ends with a discussion on self-assembled pattern formation with oxometalates.

1. Introduction

Chemistry of crystalline metal oxides is a field of diverse research interests.¹ In recent times a class of metal-oxide based clusters, called polyoxometalates (POMs), have gained significant interest due to their applications in catalysis, and in materials science in general.²⁻⁸ Polyoxometalates as the name suggests comprise of many metals, many oxygens and are usually charged and crystalline. Single molecules of POMs are usually large of the order of 1-3 nanometers and dissolve in polar solvents such as water and exist as discrete clusters in the solvent. Very recently it has been discovered that such single molecules of POMs self-assemble to form large entities with soft-matter properties.⁹⁻¹⁷ Such self-assembled

entities form a dispersed phase in a dispersing phase (solvent, usually water). They also scatter light and have a diffuse boundary. Hence following de Gennes definition of soft-matter¹⁸ these soft-states of oxometalates have been proposed to be called soft-oxometalates (SOMs).¹⁹ (Figure 1) This nomenclature facilitates to systematize and understand a burgeoning body of literature from the stand point of soft-matter or colloids. Applying the existing knowledge of soft-matter it would be possible to understand and predict the behaviour of SOMs. It is now perhaps apt to mention how we can understand the behaviour of SOMs that are beyond the crystalline regime of POMs. SOMs for instance, are not point charges. Hence Debye-Hückel approximation does not hold good for SOMs.²⁰ On the other hand their behaviour can be understood by the application of principles of short range repulsion and long range attraction as proposed by Derjaguin-Landau-Verwey-Overbeek's (DLVO) theory of stabilization of colloids.²¹ The theory states that soft-states of matter, like colloids for instance, are stabilized by the local primary and/or the secondary minima created due to the competition of repulsive electrostatic interaction and attractive van der Waals interactions in colloids. Hence it is reasonable to believe that SOMs should be charge stabilized dispersions of oxometalates. In addition to DLVO theory there is another modality of stabilization that can be envisaged with SOMs: the depletion interaction. Depletion interaction is an entropic stabilization of a colloidal system comprising of colloid-polymer mixture.²² Hence SOMs that comprise of polymers would be stabilized along the lines of depletion interaction. There is another stand-point for understanding the existence of SOMs. We know that in soft-matter physics colloids can be considered as soft-atoms which interact in a density dependent manner to give rise to various states in soft-matter. Along these lines we can envisage a number density dependent phase continuum of soft



Soumyajit Roy is at present an assistant professor (2011-till date) at Indian Institute of Science Education & Research, (IISER) Kolkata, India. Soumyajit completed his Ph.D with a summa cum laude from University of Bielefeld, Germany with Prof. Achim Müller (2005). He later moved to University of Utrecht's van't Hoff Laboratory for Physical & Colloid Chemistry, in the Netherlands, to work with Prof. Willem Kegel as a post-doctoral fellow (2005-2007). In 2007 he moved to BASF-ISIS, Strasbourg, France to work as a researcher. Before joining IISER-Kolkata he was a Professor at Changshu Institute of Technology, Jiangsu, in China.

oxometalates. In this continuum at lower extreme lies the liquid or gas like SOMs where volume fraction, $\phi < 0.2$ or alike. In the higher extreme of that continuum lies the crystalline territory of oxometalates or the crystalline POMs (for $\phi > 0.5$ or alike). From such a perspective it is possible to understand crystallization in POMs as a phenomenon of assembly of single molecular colloidal oxometalate units (or soft-atoms²³ of soft-matter) governed by a certain potential (like Baxter type potential).²⁴ Although such a view point is convenient to understand how POMs crystallize yet it is challenging to answer why in lower densities or volume fractions do the oxometalate units self-assemble to form SOMs? What drives formation of vesicle like SOMs from symmetric single molecules of POMs? We address this question in the next section. To answer this question we need to take into account the crystal structure of POMs.

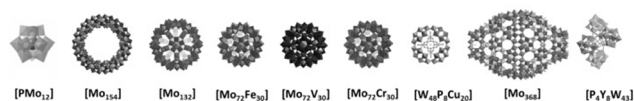


Figure 1: An overview of the POMs forming SOMs.

2. Understanding formation of SOMs from crystal structures of POMs

An intriguing aspect of self-assembly of POMs into SOMs at rather low volume fractions is what drives such assembly from already symmetric POMs to higher order sheet like structures in SOMs that fold to form giant vesicle like structure. This is so because, although spontaneous assembly of species like that of surfactants, lipids, semiconductor nanoparticles into higher order structures are ubiquitous in nature yet such spontaneous assembly is attributed to their anisotropic shapes and in cases of surfactants to their amphiphilicity.²⁵⁻²⁸ Likewise in case of semiconductor like that of CdTe, cadmium Telluride nano-particles, their truncated tetragonal shape coupled with hydrophobic and dipolar interactions lead to the formation of sheet like nanocrystals in CdTe nanocrystals. Hence in all these above cases tendency to form higher order structure can be traced to the anisotropic shapes of their constituent units and/or directional nature of interaction among those units. So the obvious question is: what drives the formation of higher order structures in SOMs from POMs? To answer this question a closer look into the crystal structure of starting POMs reveal that indeed there is an intrinsic anisotropy in the mode of packing of the clusters like that of [Mo₇₂Fe₃₀] POMs²⁹ in the crystal lattice. This anisotropy stems from the directional nature of hydrogen bonding between Fe-O...H-O-Fe linkages in the crystals.²⁹ Can such anisotropy in crystals hold the key to understand the formation of SOMs from corresponding [Mo₇₂Fe₃₀] POMs? A simulation study was performed with this end in view, where a patchy spherical model was proposed to understand the formation of SOMs.³⁰ Since each POM unit of the SOM has 30 Fe-O sites hence a model with 30 patches were proposed where each particle interacts with another particle by a single patch. (Figure 2) Each such patch size was chosen such that the transition temperature corresponds to the

energy scale of hydrogen bonding ($\sim 5-10$ kT). It was also obvious from this model that a narrow patch would induce self-assembly at higher attraction strength, while a wide patch would lead to overlap of nearby patches, destroying the point symmetry of the POM cluster or as in this case that of the sphere with the patches. The patches take care of the hydrogen bonding interaction and are represented in the model as an orientation dependent interaction. The attractive interaction between the particles is represented by a square well potential in combination with the above orientation dependent interaction. Furthermore a reduced temperature is defined as $T' = kT/\epsilon$, and the simulation is performed with 30 or 50 patchy particles in a cubic box of significantly higher length using periodic boundary conditions.³⁰ Initially random configurations are used at higher reduced temperature ($T' = 0.2$) and slowly the temperature is reduced using a well-defined cooling scheme. At higher reduced temperature a gas like configuration of the patchy spheres is observed with no order. As the temperature is reduced to $T' = 0.112$, corresponding to $\epsilon = 8.9$ kT, it is observed that the patchy particles spontaneously self-assemble into a sheet-like structure of the SOM to be formed. (Figure 3) These sheet-like structures are rather stable and it is envisaged that the entire 3D crystal is slowly formed by the self-assembly of these 2D sheets in proper orientation, formed by the patchy particles or the POM units. This structure predicted by the patchy model is furthermore consistent with the rhombohedral crystal structure observed for [Mo₇₂Fe₃₀] where 2D sheets stack perpendicular to the C₂ axis as is exactly observed to be the case from the simulation studies. When subjected to suitable synthetic conditions these sheets furthermore fold to form SOM spheres of [Mo₇₂Fe₃₀]. In the simulation study, more such 2D sheets were found to be formed when a repulsive screened Coulomb interaction was added between the patchy particles. The reason for such addition was that experimentally for stabilization of SOM vesicles it was said that the constituent POMs should carry some charge. Being charged these sheets repel each other to form crystal whereas they have ample time to fold into SOM vesicles. Such folding is also energetically favoured as it reduces the number of dangling bonds along the edges. The above explanation in short explains how SOM vesicle formation can be understood taking a closer look at the crystal structure of the starting POM and validating the formation by a patchy model where the patches are reminiscent of directional hydrogen bonding. We now ask the question, how are these SOM vesicles stabilized? Can we understand their stabilization from simple physical principles?³¹ In the next section we answer this question.

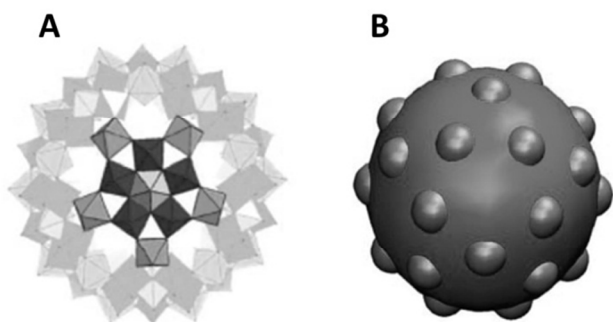


Figure 2: The patchy particle as observed from the single crystal X-ray structure of $[\text{Mo}_{72}\text{Fe}_{30}]$ (A). The patchy particle where icosidodecahedral patches are inserted on the sphere to emulate $[\text{Mo}_{72}\text{Fe}_{30}]$ cluster (B).

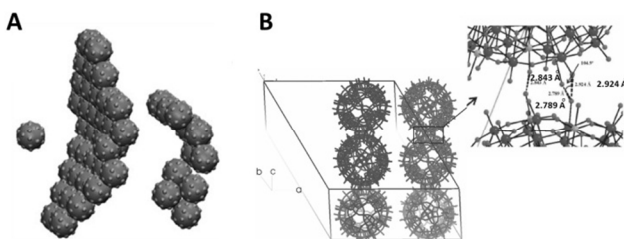


Figure 3: The 2D sheet observed from snapshots in simulation (A) and that observed in the crystal formed by differential hydrogen bonding (B). The corresponding hydrogen bonding distances between the clusters as seen from single crystal X-ray diffraction is shown at extreme right.

3. Properties of SOMs and their stabilization mechanism

SOMs have certain interesting properties. 1. They scatter light. 2. They have a diffuse or mobile boundary. 3. They are responsive to the change in the dielectric constant of the medium. Recently such a responsiveness has been found to be linear: the radii of SOM-blackberries have been found to vary inversely with the dielectric constant of the medium in cases of $[\text{Mo}_{72}\text{Fe}_{30}]$ and $[\text{Mo}_{132}]$ as model systems. (Figure 4)³² This observation is explained by a simple model. This model identifies: 1. The driving force for the formation of such SOM blackberries to be pair-wise additive attraction between the constituent POMs in the SOMs. 2. It is also found that their equilibrium size is determined by their renormalized charge density, which in turn is controlled by counter-ion condensation. It is also possible further from this model to find the interaction energy (cohesive/binding energy) that glues the POM units (each POM unit) of the SOM-blackberries together. Such energy is found to be 15 kJ/mol (at 300 K) approximately. This cohesive/binding energy is comparable to the strength of a moderate X...H...X type hydrogen bond and is thus 'soft' or supramolecular in nature.³³ It can also be said that these SOM blackberries may be justified to be called 'soft' not only because of their mobile, diffuse boundary but because of the 'soft' supramolecular nature of the interaction parameter, which is comparable in magnitude to that of moderate hydrogen bond, which in turn glue the POM units in the SOM.

We now explain this charge regulation model in more detail. Assuming the free energy G of a SOM-shell depends on two variables that are fluctuating and dependent, viz., the aggregation number, as manifested in the radius R , and the effective charge Z , we can write,

$$G/kT = 4\pi\gamma r^2 + 4\pi(2K + K') + \lambda Z^2/[2R(1+\kappa R)] - \psi Z \quad (1)$$

Here, k stands for Boltzmann's constant.

In equation (1) the first term with surface tension γ is extensive in the aggregation number and it is expected not to show up in the equilibrium equation, when we assume that the average area occupied by a POM unit in the SOM shell does not depend on R . The second term, in equation (1) with bending elastic modulus K and Gaussian modulus K' , is the curvature contribution from the Helfrich expansion of a spherical vesicle like object.³⁴ The third and fourth terms, where ψ denotes the zeta potential, regulate the effective charge of the aggregate SOM. The third term originates from the screened-Coulomb interactions on a uniformly charged sphere in the background of an electrolyte characterized by a Debye screening length $1/\kappa$, within the Debye-Hückel approximation, see:³⁵ This particular term is supposed to be correct so long we can neglect the counter ions inside the SOM-shells i.e., the case for $R \leq 1/\kappa$. The fourth term determines the extent of escape of ions from the narrow Gouy layer surrounding the SOM-shell. This term corresponds to a Legendre transformation from a constant charge—to a constant potential ensemble. See also:³⁶

Minimizing equation (1) with Z , we obtain the renormalized charge on the SOM-shell as,

$$Z = \psi R(1+\kappa R) / \lambda \quad (2)$$

Now, on substituting equation (2) in equation (1) and minimizing free energy per unit area we get the expression for R ,

$$R = 16\pi\lambda(2K+K')/\psi^2 \quad (3)$$

Since, $\lambda = e^2/4\pi\epsilon_0\epsilon kT$ and putting $\lambda = 56/\epsilon$ nm, where ϵ being the dielectric constant of the solvent, we get $R\epsilon = 1/\epsilon$, which explains the experimental observation of inverse variation of SOM-shell radius with the dielectric constant of the solvent. (Figure 4) Now, from Eulers theorem, we obtain for SOM-shells, independent of their size, at least 12 monomers on the C_5 axis of the SOM-shell are required to sit next to the predominantly present monomers on the C_6 axis. This in turn implies that each SOM-shell misses at least 12 times the cohesive bond energy, u , that monomer pairs have on the SOM-shell surface. Assuming this term to be the prime contribution, or $K' > K$, we can equate curvature energy with cohesive energy,

$$4\pi(2K + K') = -12u \quad (4)$$

Substituting equation (4) in equation (3) we get,

$$R = 48\lambda u / \psi^2 \quad (5)$$

Thus u , the cohesive energy can be obtained from the plot of R against $1/\epsilon$ and the cohesive energy so obtained is around 5-7 kT for the $[\text{Mo}_{72}\text{Fe}_{30}]$ and $[\text{Mo}_{132}]$ POMs forming the respective SOMs. This value is in close agreement with the cohesive energy obtained from the critical aggregation constant of the POMs and

thereby implying indeed the operation of a charge regulation mechanism by counter-ion condensation in the stabilization of the SOMs. This in turn implies that it is possible to control the size of the SOMs by changing the dielectric constant of the solvent. We ask in the next section: is it possible to control the overall shape and topology of the SOMs?

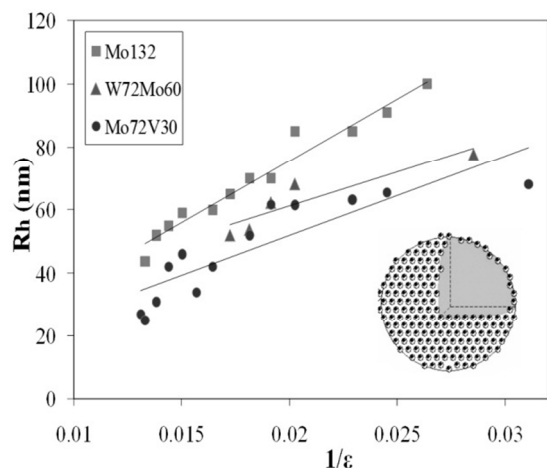


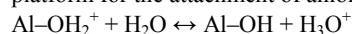
Figure 4: SOM blackberry formed by three different clusters and variation of their sizes with changing dielectric constant.

4. Directed formation of SOMs in dispersion: few examples

We turn from spontaneously generated SOMs that are held by soft, supramolecular interactions, to those numerous examples where such soft, supramolecular interactions have been employed to design Soft Oxometalates in this section. Several strategies of design have been employed. Examples include: sol-gel method,³⁷ surfactant encapsulation,³⁸ Langmuir Blodgett method,³⁹ layer-by-layer technique,⁴⁰ solvent casting,⁴¹ intercalation between layered hydroxides.⁴² These are only a few types to name. We have synthesized a class of SOMs exploiting electrostatic interactions between suitably charged colloidal templates/layered lattices/structured surfaces and POMs. It is also to be noted that a large body of literature exploring catalytic activity of POMs has employed (similar) chemical means as mentioned above for designing high surface area SOMs and the methods have been known as methods for heterogenization of POM catalysts.⁴³ Some examples of such heterogenization can be recalled, using Rh(0), Ir(0),⁴⁴ Au(0)⁴⁵ clusters, Silica,⁴⁶ MOFs (Metal organic frameworks),⁴⁷ dendrimer polyelectrolytes,⁴⁸ super-critical CO₂⁴⁹ as support. Catalytic activity of several of SOMs have also been reported. In fact it is perhaps apt to say that heterogenized POMs being dispersed oxometalates can be considered as soft-states of oxometalates. Thus such heterogenized POMs can also be treated as SOMs. More precisely, SOMs can act as model systems to understand the phenomenon of heterogenization in catalysis involving polyoxometalates. It has been proposed that such 'supported POMs' with a large surface area could act as a 'bridge' between surface catalysts and 'pseudoliquid phase' of bulk catalysts.⁵⁰ Likewise, the question as of how to obtain such high-surface area POMs in a controlled way in an aqueous solution, is important. In this section we summarize the use of electrostatic and hydrogen bond interactions to form such SOMs

as have been performed in our laboratory in recent times. We have used charged colloidal entities as structure directing agents to control the overall shape of the SOMs. Varying the shape of the colloidal cast we have been able to change the shape of the SOM. We have also shown that it is possible to use various types of POMs to make such SOMs, thereby demonstrating the applicability of the method with various POMs. Here we summarize two such cases and three examples of SOM formation with the aid of colloid.

Controlling the size and morphology of POMs in the mesoscopic regime (in the range of 100-900 nm) remains a daunting challenge. The reasons are manifold and range from: difficulty to manoeuvre the chemistry of multiple metal centers, control of pH, to overall control of the redox state of the complete system. Hence, in this regime, techniques that bypass the complex chemical crossroad and resort to the exploitation of electrostatic interaction between preformed colloidal entities as templates/scaffolds for design of mesoscopic architecture, are more successful. Such a technique is evidently supramolecular (in the sense that it involves electrostatic interactions 'beyond the chemistry of molecules'). This method also provides a platform to 'glue' molecules to form mesoscopic supramolecular architecture in the SOMs. We proposed to call this technique of using a colloidal template for forming large surface area SOMs as 'colloidal casting'. The requirements for successful colloidal casting are as follows. (1) Complementary charge between the colloidal templates and the POM (e.g., the positively charged gibbsite platelets as templates and anionic Keggin as POMs); (2) A common solvent (e.g., water). We further tested the applicability of the concept by using POMs like phosphomolybdate Keggin and [Mo₇₂Fe₃₀].⁵¹ The complementarity of charge between negatively charged [Mo₇₂Fe₃₀] and positively charged gibbsite platelets further prompted this choice. We now explain the charge complementarity. The pH of discrete [Mo₇₂Fe₃₀] clusters upon dissolving in water is around 4.5 while the isoelectric point or the point of zero charge of gibbsite is quite high, i.e., around pH 10.1. Consequently, at a pH of around 4.5, the surface of the gibbsite platelet is positively charged, (see the following equilibrium). The charged gibbsite platelet in turn acts as a platform for the attachment of anionic [Mo₇₂Fe₃₀]:



Consequently at a pH of 4.5, complementary charges on gibbsite platelets and [Mo₇₂Fe₃₀] clusters act as glue for binding them together to form hexagonal platelets of [Mo₇₂Fe₃₀] clusters.

It is also possible to change the templates from hexagonal plates to spheres. For example, using a spherical prefabricated cationic vesicle as a structure directing agent it is possible to glue simple anionic oxomolybdates by electrostatic interaction and hydrogen bonds to form large SOM super-spheres.⁵² By this method of colloidal casting, complexity can be deliberately induced in the resulting structure either through the scaffold or by means of the oxometalate. There is a high degree of control in the matter of the size and morphology of the resulting SOMs which makes this method attractive from a synthetic standpoint. For instance, it is possible to alter the SOM topology just by changing the shape of the vesicle and similar such synthetic avenues can be explored.

This specific synthesis was performed by adding an appropriate

amount of heptamolybdate to an already prepared DOTAP (a cationic fatty acid, 1,2-dioleol-3-trimethylammonium-propane) vesicle dispersion. There is a narrow window of heptamolybdate/DOTAP (M/D) concentration for formation of a stable dispersion. But, beyond this window, the dispersion becomes unstable and then it is stable again. Such a phenomenon of the formation of a stable-unstable-stable dispersion was followed experimentally by electrophoretic mobility measurements, and such experiments point to the operation of a charge inversion mechanism as the M/D concentration is varied. This is explained as follows.

Positive charge on positively charged DOTAP (D) vesicles decrease as anionic molybdates (M) are added to it and finally instability is induced for certain concentration ratio of M/D ($1.5 > M/D > 0.6$). The dispersion becomes almost zero charge and thus gets unstable. M has a charge of 6- while D has a charge of 1+. Thus if all the added Ms reside at the Ds, this instability should manifest at $M/D = 0.16$. In practice, much higher values of M/D are required to bring about this phase instability and it indicates the presence of free Ms in the dispersion. Hence, an extra amount of M (heptamolybdate) is needed to reach the unstable regime. On further addition of M (i.e., for ratio of, $10 > M/D > 3$), the dispersion again undergoes charge inversion and is now negatively charge stabilized. We can deduce analytically the interface structure of M-D SOM (Molybdate-DOTAP SOM) super-sphere from this ratio. On a closer look at the experimental results we observe that the surface charge density of both the DOTAP vesicle and that of the M-D SOM super-sphere (for $M/D \approx 3$ and higher) is same but they have opposite signs (i.e., $+5 \mu\text{mcmV}^{-1}\text{s}^{-1}$ in DOTAPs and $-5 \mu\text{mcmV}^{-1}\text{s}^{-1}$ in the composite). It is known that, a DOTAP molecule carries a unit positive charge, whereas heptamolybdate has a charge of -6. From the experimental results (i.e., taking charge inversion at $M/D \approx 3$ and higher), it follows that in the M-D SOM super-sphere for every three DOTAP molecules, there is only one heptamolybdate. This picture matches well with the surface area of DOTAP⁵³ and heptamolybdate.² So, the M-D SOM super-sphere is a vesicle of DOTAP covered with monolayer of heptamolybdate where for every three DOTAP molecules there is a heptamolybdate of the monolayer. All these SOMs are characterized by various techniques like, cryo-TEM (Transmission Electron Microscopy), TEM/EDX (TEM with Energy Dispersive X-Ray analyses), ATR-IR (Attenuated Total Reflection-Infra Red), Raman spectroscopy, Static and Dynamic Light Scattering, Small Angle X-Ray Scattering, Electrophoretic mobility measurements, potentiometric titrations, etc.

Having shown that it is possible to control the topology of the SOMs in a directed manner in dispersions we look back at spontaneously formed SOMs and ask, how does a POM interact with sound to form SOMs? We address this question in the next section.

5. Sonication and SOMs

It has been demonstrated recently that complex and large single-molecule POM clusters may even spontaneously form SOMs of colloidal size (i.e., on the order of 10-100 nm).²⁰ Of course complexity can lead to complexity but can simple precursors lead to complex colloidal entities? Now we address this question: can

very simple sparingly soluble salts of polyoxometalates, such as the ammonium salt of phosphododecamolybdate Keggin,⁵⁴ show comparable SOM superstructure formation? What happens when we sonicate a dilute solution of Keggin? It is known that dilute solutions of this Keggin salt tend to scatter light,⁵⁵ and it points to the presence of objects on colloidal length scales in the solution or more correctly in the dispersion. Recently, phosphododecatungstate Keggin is used in combination with AOT microemulsions and also as templates to synthesize fibrous, star-like, and other interesting architectures.⁵⁶ Colloidal nature of Keggin is in fact not entirely unknown, around the 1930s, complex structure formation with "phosphatide coacervates" was observed.⁵⁷ Moreover, though it was known that the ammonium salt of phosphododecamolybdate Keggin forms a colloidal dispersion in water,⁵⁵ the nature of the particles of this dispersion have not been investigated until now. However, a lot of fundamental work has been done with the ammonium phosphomolybdate Keggin.⁵⁸⁻⁷² Extensive investigations have also been carried out to explore the nature of POMs in solution⁶⁶⁻⁷² and can be traced back to 1783 to the efforts of Berzelius,⁷³ yet the nature of colloidal objects in an aqueous dispersion of the ammonium phosphomolybdate Keggin was not investigated. Hence for us to address the question of the nature of the colloidal objects in an aqueous dispersion of $[\text{PMo}_{12}]$ Keggin ($[\text{PMo}_{12}\text{O}_{40}]^{3-}$, Keggin) we started our investigation with a very dilute sonicated dispersion of the ammonium salt of the POM. This investigation reveals that a sonicated aqueous colloidal dispersion of $[\text{PMo}_{12}]$ Keggin shows spontaneous formation of small spheres of $[\text{PMo}_{12}]$ Keggin and its lacunary analogues (5-50 nm radii). These nano-spheres ripen in an Ostwald ripening like regime and finally after 2-3 days generate stable micrometer sized "pea-pod"-like mesoscopic SOM-particles. (Figure 5) These peapods are structurally heterogeneous and comprise of $[\text{P}_2\text{Mo}]$ ($[\text{P}_2\text{MoO}_{11}]^{6-}$) spheres sheathed by a MoO_3 nanorod. Upon acidification the spheres leech out leaving behind only rods of MoO_3 . This entire investigation was carried out using time-resolved dynamic light scattering (DLS), transmission electron microscopy (TEM), and scanning TEM (STEM) with a high-angle annular dark field detector (HAADF) for energy dispersive X-ray (TEM/EDX) elemental analyses.

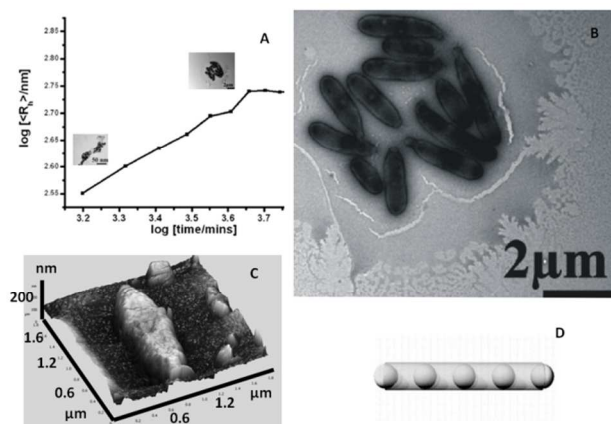


Figure 5: a) Ripening of the $[\text{PMo}_{12}]$ spheres in a sonicated dispersion into peapods with time. b) TEM image of peapods. c) AFM image of a peapod. d) A model of a peapod.

We now speculate why peapods are formed. It is relatively easy from energy requirement point of view to understand the formation of a cylindrical morphology rather than a sphere. This is because in case of a cylinder, unlike a sphere, there is no requirement for the generation of 12 C_5 axes and the breaking of 12 contacts thereof. The next question as of why spherical $[P_2Mo]$ forms spheres and remain wrapped in a sheet of MoO_3 is yet to be answered. The story is more interesting from a single molecule chemistry point of view. From such a chemical point of view it is intriguing to see how upon sonication the less-soluble ammonium salt of two component $[PMo_{12}]$ Keggin goes back to its two starting components, MoO_3 sheet and PO_4^{3-} , spheres in $[P_2Mo]$ via a series of shape transitions. Though we do not understand the exact mechanism of this shape transition, we may still allude to an architectural concept for stress analysis. It is known that any architecture or any structure breaks along the weaker lines of its construction when it is subjected to a yielding force. Similarly we may say that the phenomenon as outlined here traces out the weaker fault lines of $[PMo_{12}]$ Keggin's molecular construction. Needless to say those fault-lines in Keggin link the central tetrahedral phosphate with the four surrounding $[Mo_3]$ caps. More precisely those are the μ_3 -Os along which the Keggin decomposes, forming macroscopic peapods. The reason for stress along this fault-line we believe is due to the two different intrinsic curvatures preferred by two types of chemical motifs, viz., the PO_4 and MoO_3 caps. Moreover, the Mo-O-Mo angular strain in the starting Keggin is released as thermodynamically more stable spherical $[P_2Mo]$ species are formed within the peapods. We also believe that this strain on a molecular scale leads to the thermodynamic instability of the starting Keggin and ultimately results in the formation of a thermodynamically stable macroscopic composite, the peapods. But for this stress to be more active it is essential that the starting molecule is insoluble. Since the phenomenon described here leads to the formation of new shapes (on macroscopic length scales) as a result of degeneration (on a molecular scale), we propose to name this phenomenon as "degenerative morphogenesis". In contrast to the larger clusters, the smaller and less-soluble salts of POMs, such as that of the ammonium salt of the phosphomolybdate Keggin discussed here, do not show spherical SOM-shell-like superstructures, instead, they show peapod-shaped SOM formation as shown here. Now we ask: can we induce controlled motion in these peapods, whose constitution is known down to the last atom? In the next section we answer this question.

6. SOMs in motion with light

Living systems use motor proteins to actively transport ingredients over large distances.⁷⁴ Clearly synthetically emulating such a process would require two steps: (1) Controlled generation of mesoscopic objects starting from well-defined precursors; (2) Using physical means to induce controlled motion in such mesoscopic objects. This is where SOMs especially SOM peapods can come into play. Being endowed with an optical axis it can be responsive to variations in external optical fields. It is hence reasonable to envisage that a SOM-peapod with a responsive component to an external optical perturbation can be a

synthetic model system showing controlled motion comparable to biological systems. Furthermore, could we actually move the SOM in a complex pre-designed path by known amounts? To answer this question, we designed such a path using optical forces, and an optically responsive SOM-peapod was made to move along that path in our model system. The optical forces were exerted by optical tweezers. Optical tweezers can confine single mesoscopic particles and can apply controlled forces ranging from few to several hundred pN.⁷⁵ It was thus an ideal candidate to induce controlled motion in SOMs. Translation of trapped SOMs linearly by translating the optical trap is easy and can be done, but translation along more complex paths which may be required to emulate biological processes are not simple and are shown by us. In our method, the trapped particle is moved by changing the angle of polarization of the input trapping beam (linearly polarized). This enables us to completely control the motion both in terms of stopping the particle or changing its velocity. We are also able to rotate the particles exploiting spin-orbit interactions of light affecting the distribution of the electric field inside the sample chamber.⁷⁶ (Figure 6) The enhanced spin-orbit interaction can be induced in the sample chamber using thicker cover-slips (thickness 250 μm) than the conventional ones used in optical tweezers (130 - 160 μm). Since peapods are asymmetric birefringent particles with a preferred optic axis they can line up with the polarization of the trapping beam. We have also designed rather exotic optical potential in our optical trap in order to induce controlled micro-optomechanics on individual pea-pod SOMs. The details on the design of optical potential is reported by us elsewhere.⁷⁷ We ask, using light-SOM interaction what else might be possible? SOMs have LMCT (Ligand-Metal Charge Transition) transitions. Is it possible to exploit such responsiveness of SOMs to light to self-assemble them and write patterns using light? In the next section we address this question.

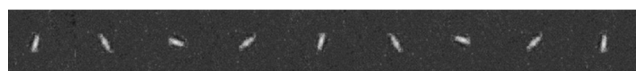


Figure 6: Snap shots of rotation of peapods in an optical trap.

7. Self-assembly and patterning of SOMs by light

The beauty of self-assembly is often the level of complexity and high specificity that can be obtained in the final structures with minimum dissipation of energy, thus ensuring high efficiency. Self-assembly strategies in nature have been extensively studied and applied by scientists in the meso-scale for diverse applications in nano-technology,⁷⁸⁻⁸² molecular electronics,⁸³ etc. Inducing self-assembly by an external stimulus is especially interesting,⁸⁴ as it allows control of the final structures by alteration of the parameters of the applied stimulus. Light, and SOMs for this reason, are ideal choice in this matter. This is so because as an external stimulus, light can be tuned. SOMs are responsive to light and thus the entire light induced SOM assembly, if generated can be tuned altogether. It is worth noting that light assisted self-assembly has led to novel materials,⁸⁵⁻⁸⁷ for sensing,⁸⁸ delivery,⁸⁹ optics⁹⁰ applications. We were able to prepare SOM nanotubes with LMCT transitions that enable them

to be responsive to stimulation by laser light of 1064 nm and exploiting this responsiveness we were able to pattern SOMs to form higher ordered crystalline structures to be described here.

Before we proceed further it is worth reviewing the literature on reversible and irreversible self-assembly by light in a bit more detail. Our patterning of SOMs by light is an irreversible patterning induced by light. Induced self-assembly are of two types: reversible self-assembly (where the assembly is lost on removal of stimulus) and irreversible (where permanent self-assembled structure is formed). Concentration dependent reversible and irreversible assembly of nanoparticles have been shown.⁹¹ Multi-scale patterning using directed fields has been achieved also recently though continuous patterning has proven elusive.⁹² For instance, patterned chains and networks of gold nanocrystals have been formed. Likewise, formation of colloidal crystals by a directed electric field using bubble-mediated nucleation⁹³ or more recently, single crystals of glycine⁹⁴ that have been grown from solution have been achieved due to the formation of a 'hot spot' or high temperature region produced by a laser beam focused on a gold surface. We ask, is it possible to create similar hot spots and induce a bubble mediated SOM assembly that would ultimately self-assemble and crystallize forming patterns at our volition?

To do so, we synthesize SOM nanotubes with LMCT transition tuned to the wavelength of our thermo-optic trapping laser. We focus the thermo-optic trapping laser on a dispersion of SOM nanotubes. Due to LMCT type transitions the laser irradiation excites the dispersion and creates a bubble with SOMs. (Figure 7) Due to buoyant forces this bubble levitates to the base of sample chamber. Due to difference in surface energy between the surface and the base of the bubble, a convection current sets in, which draws SOM nanotubes from the bulk dispersion to the base of the bubble. Now we move the sample chamber by moving the microscope stage and this leads to two possibilities for the bubble, viz., generation of a new bubble or migration of the generated bubble with the laser. In fact second option is energetically more favoured and consequently the bubble moves with the laser depositing SOMs on the base of the sample chamber which later undergoes nucleation to give crystals of oxometalates. Hence by moving the sample chamber or more precisely the microscope stage we can write any continuous pattern we want with SOMs which in turn nucleates forming patterns of crystalline oxometalates. In this way we have formed patterns using: 1) soft-oxometalate nanotubes⁹⁵ having comparatively high absorbance at $\lambda = 1064$ nm resulting from a Ligand Metal Charge Transfer (LMCT) type transition, and 2) paracetamol, fluorescent dyes (such as perylene where the pattern can be illuminated under light) and carbon nanotubes (CNTs) loaded on the SOMs, where SOM helps in inducing nucleation. We observe that continuous patterns can indeed be formed using the SOMs, at much lower powers than that typically employed in laser induced nucleation.⁹⁶⁻⁹⁸ Patterns are also formed using organic molecules anchored on the SOMs, we observe assisted nucleation exploiting the excitation of SOM core due to LMCT type transition when exposed to the intense trapping beam. The organic molecules are chosen keeping in mind the presence of hydrogen bonding and coordination sites. This technique is much simpler, easily controllable and fast for any optical patterning

scheme and provides a facile way for forming SOM or oxometalate based arrays for various catalytic and materials science applications. In short starting from crystalline POMs we can make SOMs, self-assemble them under light and write patterns of crystalline oxometalates thereof.

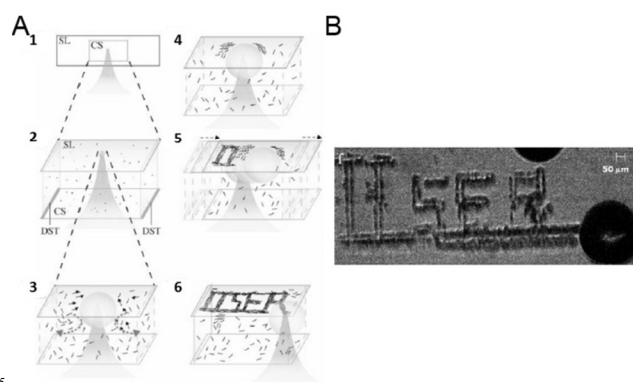


Figure 7: Thermo-optic trapping of SOM nanotubes: (A) focusing of the laser in the SOM dispersion to form the hot-spot is shown (1). The hot-spot leads to the formation of the bubble (2). Gibbs-Marangoni convection of the SOMs from the dispersion to the base of the bubble takes place (3). Accumulation of SOMs at the base of the bubble or on the surface of the glass slide takes place (4). Moving the laser focus moves the bubble to a new spot and same phenomena as shown in figures 1-4 is repeated (5). This way patterns can be written. The pattern 'IISER' written on the glass slide is shown schematically (6). The real pattern of 'IISER' from the experiment is shown in the right (B).

8. Conclusion

To conclude, we have shown that starting from crystalline POMs we can transcend the crystalline boundary and enter into the territory of liquid/soft-matter by making SOMs. SOMs can be considered as units of oxometalates with a diffuse boundary constituting oxometalates in soft/liquid state. As we increase the volume fraction/concentration/number density of SOMs it is possible to induce a phase transition from liquid to crystalline regime. It is in this way we can envisage crystallization of POMs which is still not well-understood by invoking the SOM model to describe it.⁹⁹ We have also shown that at very low concentration regime SOMs are self-assembled and their assembly can be understood from a patchy model constructed from the consideration of the crystal structure of the corresponding POMs. Self-assembly of SOMs is not confined to complex POM precursors but they can be assembled from simple POM units as well. We have shown the sonication induced self-assembly of SOM peapods and have shown their controlled motion in an optical field. We have further shown exploitation of SOM-light interaction in making self-assembled patterns of SOMs with light which in turn undergoes nucleation and crystallization. Starting from crystalline POMs we have explored the world of soft-matter with SOMs and have patterned them with light in a controlled way to get back to crystalline oxometalates to conclude our journey. Needless to say the journey with SOMs is just beginning.

Acknowledgement

The author thanks Preethi Thomas and Subharanjan Biswas for their help and Prof. Tianbo Liu for kindly providing raw materials for figures 1 and 4 and Dr. Ethayaraja Mani for providing raw materials for figure 2. DST fast-track, BRNS-DAE grants and IISER-Kolkata are thanked for financial support.

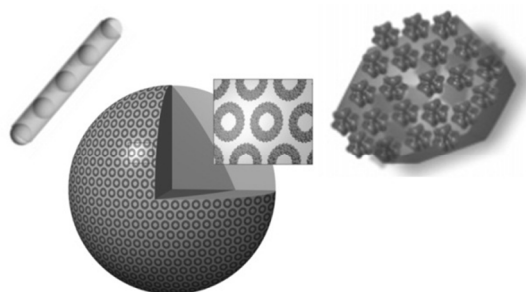
Notes and references

Eco-Friendly Applied Materials Laboratory (EFAML), Materials Science Centre, Department of Chemical Sciences, Indian Institute of Science Education and Research-Kolkata (IISER-Kolkata), Mohanpur Campus, Mohanpur-741252, India. E-mail: s.roy@iiserkol.ac.in, roy.soumyajit@googlemail.com.

1. J. L. G. Fierro, *Metal oxides: Chemistry & Applications*, CRC Press, Boca Raton, 2006.
2. M. T. Pope, *Heteropoly and Isopoly Oxometalates*, Springer, Berlin, 1983.
3. C. L. Hill, (ed.) *Chem. Rev. Thematic Issue on Polyoxometalates*, 1998, **98**.
4. M. T. Pope, A. Müller, *Angew. Chem., Int. Ed. Engl.*, 1991, **30**, 34.
5. A. P. Ginsberg, (ed.) *Inorganic Synthesis*, 1990, **27**, 71.
6. *Comprehensive Coordination Chemistry*, ed. L. Cronin, J. A. McCleverty, T. J. Meyer, Elsevier, Amsterdam, 2004.
7. *Polyoxometalate Chemistry for Nanocomposite Design*, ed. T. Yamase, M. T. Pope, Kluwer Academic Publishers, New York, 2002.
8. *Introduction to Polyoxometalate Chemistry : From Topology via Self-Assembly to Applications*, ed. M. T. Pope, A. Müller, Kluwer Academic Publishers, New York, 2001.
9. (a) A. Müller, S. K. Das, V. P. Fedin, E. Krickemeyer, C. Beugholt, H. Bögge, M. Schmidtman, B. Z. Hauptfleisch, *Z. Anorg. Allg. Chem.*, 1999, **625**, 1187. (b) A. M. Müller, C. Serain, *Acc. Chem. Res.*, 2000, **33**, 2.
10. A. Müller, E. Krickemeyer, H. Bögge, M. Schmidtman, F. Peters, *Angew. Chem., Int. Ed.*, 1998, **37**, 3360.
11. A. Müller, S. Sarkar, S. Q. N. Shah, A. X. Trautwein, V. Schünemann, *Angew. Chem., Int. Ed.*, 1999, **38**, 3238.
12. B. Botar, P. Kögerler, C. L. Hill, *Chem. Commun.*, 2005, **25**, 3138.
13. A. M. Todea, A. Merca, H. Bögge, J. van Slageren, M. Dressel, L. Engelhardt, M. Luban, T. Glaser, M. Henry, A. Müller, *Angew. Chem., Int. Ed.*, 2007, **46**, 6106.
14. (a) S. S. Mal, U. Kortz, *Angew. Chem., Int. Ed.*, 2005, **44**, 3777. (b) D. Jabbour, B. Keita, L. Nadjo, U. Kortz, S. S. Mal, *Electrochem. Comm.*, 2005, **7**, 841. (c) M. S. Alam, V. Dremov, P. Müller, A. V. Postnikov, S. S. Mal, F. Hussain, U. Kortz, *Inorg. Chem.*, 2006, **45**, 2866.
15. A. Müller, E. Beckmann, H. Bögge, M. Schmidtman, A. Dress, *Angew. Chem., Int. Ed.*, 2002, **41**, 1162.
16. R. C. Howell, F. G. Perez, S. Jain, W. H. Dew, A. L. Rheingold, L. C. Francesconi, *Angew. Chem., Int. Ed.*, 2001, **113**, 4155.
17. (a) A. Müller, E. Diemann, C. Kuhlmann, W. Eimer, C. Serain, T. Tak, A. Knöchel, P. K. Pranzas, *Chem. Commun.* 2001, 1928. (b) T. Liu, E. Diemann, H. Li, A. Dress, A. Müller, *Nature*, 2003, **426**, 59.
18. P. -G. de Gennes, *Soft Interfaces*, Cambridge University Press, Cambridge, 1997.
19. S. Roy, *Comm. Inorg. Chem.*, 2011, **32**, 113.
20. T. Liu, *Langmuir*, 2010, **26**, 9202.
21. H. Lyklema, *Fundamentals of Interface and Colloid Science*, Elsevier Academic Press, Wageningen, 2004, vol. 1-5.
22. A. Vrij, *Pure & Appl Chem.*, 1976, **48**, 471.
23. W. Poon, *Science*, 2004, **304**, 830.
24. P. Prinsen, T. Odijk, *J. Chem. Phys.*, 2004, **121**, 6525.
25. A. Patti, M. Dijkstra, *Phys. Rev. Lett.*, 2009, **102**, 128301.
26. J. Israelachvili, *Intermolecular and Surface Forces*, Academic, San Diego, CA, 1992.
27. Z. Tang, Z. Zhang, Y. Wang, S. C. Glotzer, N. Kotov, *Science*, 2006, **314**, 274.
28. Z. Zhang, S. C. Glotzer, *Nano Lett.*, 2004, **4**, 1407.
29. A. Müller, *Angew. Chem., Int. Ed.*, 1999, **38**, 3238.
30. E. Mani, E. Sanz, S. Roy, M. Dijkstra, J. Groenewold, W. K. Kegel, *J. Chem. Phys.*, 2012, **136**, 144706.
31. A. A. Verhoeff, M. L. Kistler, A. Bhatt, J. Pigga, J. Groenewold, M. Klokkenburg, S. Veen, S. Roy, T. Liu, W. K. Kegel, *Phys. Rev. Lett.*, 2007, **99**, 066104.
32. A. Müller, S. Roy, *Oxomolybdates: From Structures to Functions in a New Era of Nanochemistry. In The Chemistry of Nanomaterials: Synthesis, Properties and Applications*, ed. C. N. R. Rao, A. Müller, A. K. Cheetham, Wiley-VCH, Weinheim, 2005, 452.
33. G. A. Jeffrey, *An Introduction to Hydrogen Bonding*, Oxford University Press, New York, 1997.
34. W. Helfrich, *Z. Naturforsch.* 1973, **28c**, 693.
35. R. J. Hunter, *Foundations of Colloid Science*, Oxford University Press, New York, 2nd Ed., 2001.
36. R. P. Feynman, R. B. Leighton, M. L. Sands, *The Feynman Lectures on Physics—Commemorative Issue*, Addison-Wesley, Redwood CA, Vol. II, 1989.
37. S. Polarz, B. Smarsley, C. Göltner, M. Antonietti, *Adv. Mater.*, 2000, **12**, 1503.
38. (a) D. G. Kurth, P. Lehmann, D. Volkmer, H. Cölfen, M. J. Koop, A. Müller, A. Du Chesne, *Chem. Eur. J.*, 2000, **6**, 385. (b) D. Volkmer, A. Du Chesne, D. G. Kurth, H. Schnablegger, P. Lehmann, M. J. Koop, A. Müller, *J. Am. Chem. Soc.*, 2000, **122**, 1995. (c) D. G. Kurth, P. Lehmann, D. Volkmer, A. Müller, D. Schwahn, *J. Chem. Soc., Dalton Trans.*, 2000, 3989.
39. (a) M. Clemente-León, C. Mingotaud, B. Agricole, C. J. Gómez-García, E. Coronado, P. Delhaës, *Angew. Chem., Int. Ed.*, 1997, **36**, 1114. (b) M. Clemente-León, B. Agricole, C. Mingotaud, C. J. Gómez-García, E. Coronado, P. Delhaës, *Langmuir*, 1997, **13**, 2340.
40. S. W. Keller, H.-N. Kim, T. E. Mallouk, *J. Am. Chem. Soc.*, 1994, **116**, 8817.
41. I. K. Song, M. S. Kaba, G. Coulston, K. Kourtakis, M. A. Barreau, *Chem. Mater.*, 1996, **8**, 2352.
42. T. Kwon, T. J. Pinnavaia, *J. Mol. Catal.*, 1992, **74**, 23.
43. (a) *Catalysts for Fine Chemicals Synthesis: Catalysis by Polyoxometalates*, ed. I. V. Kozhevnikov, J. Wiley & Sons, Chichester, 2002. vol. 2. (b) N. Mizuno, M. Misono, *Chem. Rev.*, **1998**, **98**, 199. (c) R. Neumann, A. M. Khenkin, *Chem. Commun.*, 2006, 2529. (d) R. G. Finke, S. Özkar, *Coord. Chem. Rev.*, 2004, **248**, 135.
44. Y. Wang, A. Neyman, E. Arkhangelsky, V. Gitis, L. Meshi, I. A. Weinstock, *J. Am. Chem. Soc.*, 2009, **131**, 17412.
45. (a) N. M. Okun, T. M. Anderson, C. L. Hill, *J. Am. Chem. Soc.*, 2003, **125**, 3194. (b) N. M. Okun, M. D. Ritorto, T. M. Anderson, C. L. Hill, *Chem. Mater.*, 2004, **16**, 2551.
46. (a) C.-Y. Sun, S.-X. Liu, D.-D. Liang, K.-Z. Shao, Y.-H. Ren, Z.-M. Su, *J. Am. Chem. Soc.*, 2009, **131**, 1883. (b) A. Corma, H. García, F. X. L. Xamena, *Chem. Rev.*, 2010, **110**, 4606.
47. (a) L. Plault, A. Hauseler, S. Nlate, D. Astruc, J. Ruiz, S. Gataud, R. Neumann, *Angew. Chem., Int. Ed.*, 2004, **43**, 2924. (b) S. Nlate, D. Astruc, R. Neumann, *Adv. Synth. Catal.*, 2004, **346**, 1445.
48. G. Maayan, B. Ganchegui, W. Leitner, R. Neumann, *Chem. Commun.*, 2006, 2230.
49. I. V. Kozhevnikov, *Chem. Rev.*, 1998, **98**, 171.
50. (a) S. Roy, M. C. D. Mourad, M. T. Rijneveld-Ockers, *Langmuir*, 2007, **23**, 399. (b) S. Roy, H. J. D. Meeldijk, A. V. Petukhov, M. Versluijs, F. Soulimani, *Dalton Trans.*, 2008, 2861.
51. S. Roy, L. C. A. M. Bossers, H. J. D. Meeldijk, B. W. M. Kuipers, W. K. Kegel, *Langmuir*, 2008, **24**, 666.
52. J. Generosi, C. Castellano, D. Pozzi, A. C. Castellano, R. Felici, F. Natali, G. Fragneto, *J. Appl. Phys.*, 2004, **96**, 6839.

54. (a) J. F. Keggin, *Nature*, 1933, **131**, 908. (b) J. F. Keggin, *Proc. R. Soc. London, Ser. A*, 1934, **144**, 75.
55. A. I. Vogel, *Qualitative Inorganic Analysis; Longman Scientific and Technical*, Essex, England, 1987.
56. (a) M. Li, S. Mann, *Langmuir*, 2000, **16**, 7088. (b) D. Rautaray, S. R. Sainkar, M. Sastry, *Langmuir*, 2003, **19**, 10095. (c) S. Mandal, D. Rautaray, M. Sastry, *J. Mater. Chem.*, 2003, **13**, 3002. (d) Z. Xin, J. Peng, T. Wang, B. Xue, L. Li, E. Wang, *Inorg. Chem.*, 2006, **45**, 8856.
57. B. de Jong H. G., *Colloid Science*, ed. H. R. Kruyt, Elsevier, Amsterdam, 1949.
58. T. Ueda, T. Toya, M. Hojo, *Inorg. Chim. Acta.*, 2004, **357**, 59.
59. X. López, J. Maestre, C. Bo, J.-M. Poblet, *J. Am. Chem. Soc.* 2001, **123**, 9571.
60. M. Janik, B. Bardin, R. Davis, M. J. Neurock, *Phys. Chem. B*, 2006, **110**, 4170.
61. C. Rocchiccioli-Deltcheff, A. Aouissi, M. Bettahar, S. Launay, M. J. Fournier, *Catal.* 1996, **164**, 16.
62. N. Mizuno, M. Misono, *Chem. Rev.*, 1998, **98**, 199.
63. I. V. Kozhevnikov, *Chem. Rev.*, 1998, **98**, 171.
64. C. Hill, C. M. Prosser-McCartha, *Coord. Chem. Rev.*, 1995, **143**, 407.
65. X. López, C. Nieto-Draghi, C. Bo, J. Avalos, J. -M. Poblet, *J. Phys. Chem. A*, 2005, **109**, 1216.
66. A. Müller, C. Seraine, *Acc. Chem. Res.*, 2000, **33**, 2.
67. A. Müller, S. Roy, *Coord. Chem. Rev.*, 2001, **245**, 153.
68. M. Pope, G. Varga Jr., *Inorg. Chem.*, 1966, **5**, 1249.
69. M. Baker, P. Lyons, S. Singer, *J. Am. Chem. Soc.*, 1955, **77**, 2011.
70. I. Validzic, G. van Hooijdonk, S. Oosterhout, W. Kegel, *Langmuir*, 2004, **20**, 3435.
71. T. Kurucsev, A. Sargeson, B. West, *J. Phys. Chem.*, 1957, **61**, 1567.
72. K. Tytko, U. Trobisch, *Gmelin Handbook of Inorganic Chemistry*, ed. H. Katscher, Springer-Verlag, Berlin, 1986, B3a, 40.
73. J. Berzelius, *Poggend Ann. Phys. Chem.* 1826, **6**, 1206.
74. B. Alberts, A. Johnson, J. Lewis, M. Raff, K. Roberts, P. Walter, *Molecular Biology of the Cell*, Garland Science, New York, 2002.
75. T. T. Perkins, *Laser & Photon. Rev.*, 2008, **3**, 203.
76. A. Haldar, S. Pal, B. Roy, S. D. Gupta and A. Banerjee, *Phys. Rev. A*, 2012, **85**, 033832.
77. B. Roy, A. Sahasrabudhe, B. Parasar, N. Ghosh, P.K. Panigrahi, A. Banerjee, S. Roy, *J. Mol. Eng. Mat.*, 2014 (under revision).
78. T. Leong, Z. Gu, T. Koh, D. H. Gracias, *J. Am. Chem. Soc.*, 2006, **128**, 11336.
79. J. C. Love, A. R. Urbach, M. G. Prentiss, G. M. Whitesides, *J. Am. Chem. Soc.*, 2003, **125**, 12696.
80. Z. Gu, Y. Chen, D. H. Gracias, *Langmuir*, 2004, **20**, 11308.
81. J. Erlebacher, M. J. Aziz, A. Karma, N. Dimitrov, K. Sieradzki, *Nature*, 2001, **410**, 450.
82. J. S. Lindsey, *New J. Chem.*, 1991, **15**, 153.
83. D. Roy, J. N. Cambre, B. S. Sumerlin, *Prog. Polym. Sci.*, 2010, **35**, 278.
84. M. Fialkowski, K. J. M. Bishop, R. Klajn, S. K. Smoukov, C. J. Campbell, B. A. Grzybowski, *J. Phys. Chem. B*, 2006, **110**, 2482.
85. A. J. Kim, P. L. Biancaniello, J. C. Crocker, *Langmuir*, 2006, **22**, 1991.
86. U. Dassanayake, S. Fraden, A. van Blaaderen, *J. Chem. Phys.*, 2000, **112**, 3851.
87. M. Oh, C. A. Mirkin, *Nature*, 2005, **438**, 651.
88. F. Ecole, T. P. Davisa, R. A. Evans, *Polym. Chem.*, 2010, **1**, 37.
89. D. L. J. Vossen, D. Fific, J. Penninkhof, T. van Dillen, A. Polman, A. van Blaaderen, *Nano Lett.* 2005, **5**, 1175.
90. R. Klajn, K. J. M. Bishop, P. A. Grzybowski, *Proc. Natl. Acad. Sci.*, 2007, **104**, 10305.
91. M. Grzelczak, J. Vermant, E. M. Furst, L. M. Liz-Marzán, *ACS Nano*, 2010, **4**, 3591.
92. S. J. Zhen, Z. Y. Zhang, N. Li, Z. D. Zhang, J. Wang, C. M. Li, L. Zhan, H. L. Zhuang, C. Z. Huang, *Nanotechnology*, 2013, **24**, 055601.
93. T. Uwada, S. Fuji, T. Sugiyama, A. Usman, A. Miura, H. Masuhara, K. Kanaizuka, M. Haga, *ACS Appl. Mater. Interfaces*, 2012, **4**, 1158.
94. S. Fujii, K. Kanaizuka, S. Toyabe, K. Kobayashi, E. Muneyuki, M.-A. Haga, *Langmuir*, 2011, **27**, 8605.
95. B. Roy, M. Arya, P. Thomas, J. K. Juergschat, K. V. Rao, A. Banerjee, C. M. Reddy, S. Roy, *Langmuir*, 2013, **29**, 14733.
96. T. Sugiyama, K. Yuyama, H. Masuhara, *Acc. Chem. Res.*, 2012, **45**, 1946.
97. B. A. G. X. Sun, A. S. Myerson, *Cryst. Growth Des.*, 2006, **6**, 684.
98. J. M. J. Zaccaro, A. S. Myerson, B. A. Garetz, *Cryst. Growth Des.*, 2001, **1**, 5.
99. D. Rosenbaum, P. C. Zamora, C. F. Zukoski, *Phys. Rev. Lett.*, 1996, **76**, 150.

5 Table of Content



10